Chapter 3

Forensic Potential of Atomic Force Microscopy with Special Focus on Age Determination of Bloodstains

Threes Smijs and Federica Galli

Additional information is available at the end of the chapter

http://dx.doi.org/10.5772/intechopen.77204

Abstract

An important aspect of any crime scene investigation is to detect, secure and analyze trace evidence. In forensic examinations where topographic characterization is important like in fingermark, textile and document forgery examinations, the atomic force microscopy (AFM) imaging technique can be of value. However, it is the force spectroscopy that could make AFM a versatile tool in crime investigations. Particularly, the ability to measure changes in mechanical properties of forensic trace material over time makes this technology in potential interesting for forensic examinations. The usefulness of force measurements to evaluate the elasticity of red blood cells (RBCs) in relation to the age of a bloodstain is an interesting example. With minimally invasive AFM technology, time-dependent alterations in the viscoelasticity of RBCs that occur during the aging of bloodstains can be featured. A discrimination between traces left by the perpetrator and other persons that have been present at the crime scene will thus be enabled. A recently obtained proof-of-concept demonstrating the usefulness of AFM for age estimation of bloodstains will be described. Additionally, the usefulness of AFM imaging and force spectroscopy for human hair, document forgery, textile fiber, fingermark and gunshot and explosive residue examinations will be discussed.

Keywords: forensic, atomic force, crime, red blood cell, textile, fingermark, explosives, forgery

1. Introduction

During a crime scene investigation (CSI), it is essential to detect, secure and interpret biological and nonbiological traces [1, 2]. The physical and chemical procedures for these forensic examinations can be performed in the laboratory but are also carried out more and more at the scene of the crime. Especially, the biological traces that can be used for DNA-profiling are important.

Crucial condition thereby is the use of non- to minimally invasive methods. Key information regarding offenses may thus be established and contribute to the reconstruction of crimes.

Today different nanotechnologies such as the application of nanoscale powders, high-resolution transmission and scanning electron microscopy (HRTEM, HRSEM) and atomic force microscopy (AFM) are available for forensic investigations [3, 4]. However, forensic trace characterization at the nanoscale may not necessarily yield relevant forensic information as explained by Inman and Rudin with the principle of divisible matter [5, 6]. Relevant forensic materials thus need to be found and interpreted preferable at the dimension at which they are created. Nanoscale, extremely detailed information may be superfluous and not related to evidence. Nevertheless, it has been demonstrated that high-resolution scanning probe AFM has interesting forensic applications [7, 8]. This chapter focuses on the forensic potential of AFM with special focus on the force measurements, known as force spectroscopy (FS). First, AFM imaging and FS are briefly explained. Second, the forensic potential of AFM imaging and FS is evaluated with special attention to age determination of bloodstains. Third, a conclusion is provided based on the effectiveness and usefulness of the information provided by this technology in relation to the system of criminal justice.

2. Principles of AFM

An AFM consists of a cantilever with a tip at the end, together named the probe, a piezo-electric XY- and Z- scanner, a laser and a photo-diode detector system (see **Figure 1**) and can be operated in different modes. In the contact mode, the tip is dragged across the surface at constant force, in the intermittent contact mode the cantilever is oscillating and the tip will be repulsed at the lowest oscillation point and get out of contact at the upper part of the oscillation, in the non-contact mode the cantilever is oscillating close to the sample but without contacting its surface and in the force modulation mode the tip is oscillating while remaining in contact with the sample surface [9].

2.1. AFM imaging

Briefly, a sample is scanned by the tip (mostly sharp and made of silicon or silicon nitride) parallel to the sample surface (with the XY-scanner) while interactions between sample and probe are experienced. These interactions concern attractive and repulsive forces between molecules of the sample and tip thereby causing deflections of the cantilever toward or away from the sample that results in a deflection of the laser beam and can be recorded by a photo-diode system (see **Figure 1**). As the deflection of the cantilever is directly proportional to the force, a feedback system is usually employed. With this feedback system, the height of the cantilever is adjusted in order to maintain a constant deflection (force) while moving parallel to the surface. In this way an image of the topography of a sample, a height image, is created, and quantitative surface roughness can be determined from height images. In another type of imaging, phase imaging, the phase shift between the driving signal and the cantilever signal as it interacts with the surface is recorded during intermittent contact AFM or noncontact

http://dx.doi.org/10.5772/intechopen.77204

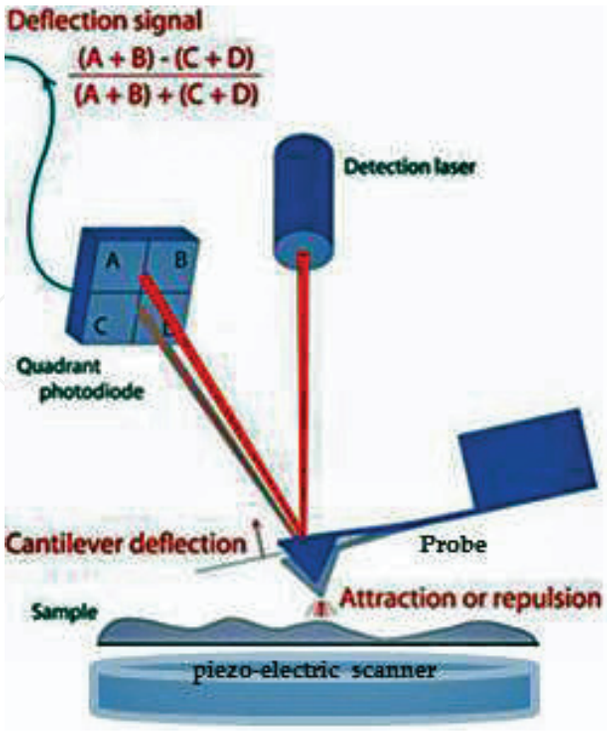

Figure 1. Illustration (kindly provided by JPK Instruments AG) of the basic components of an AFM, the probe, piezo-electric scanner, the laser, sample and photo-diode detector system. Depending on the roughness of the surface and type of measurements, the tip can be pyramid-shaped (commonly made of silicon or silicon nitride) with a curvature radius ranging from 2 nm to 2 μm or spherical (0.5–2.5 μm in diameter and mostly made of titanium or silica). Force interactions between tip and surface molecules will result in a deflection of the cantilever that is recorded as the deflection of a laser beam aligned to the back of the cantilever. Quadrant photo-diodes (with optically active areas A, B, C and D) will then convert the laser signals into an electrical output signal that is proportional to the deflection of the cantilever.

AFM. In intermittent contact, in AFM mode, the cantilever is oscillating and the tip is repulsed at the lowest oscillation point and get out of contact at the upper part of the oscillation. The phase lag is caused by the energy dissipation in the cantilever because of the experienced interaction forces between probe and sample. Dissipation differs for different materials; therefore, the phase image can provide extensive information on differences in sample composition, particularly on flat surfaces.

2.2. Force spectroscopy

In case of force measurements, the probe is moved vertically toward the sample and subsequently retracted. As the tip further approaches the surface attractive, mostly van der Waals, forces become significant. These interactions result in a "snap-to-contact" of the tip with the sample followed by a deflection away caused by repulsive molecular interactions. In this regime, the sample is indented on purpose. From the resulting force-distance curve (FD, see for a schematic representation **Figure 2**), cantilever properties and contact area nanomechanical properties such as a material's modulus of elasticity, the Young's modulus (YM), can be quantitatively obtained. The YM is a mechanical property that indicates the force per unit area that is needed to compress or stretch an elastic material. Stiffer materials have larger YM. This contact stiffness can

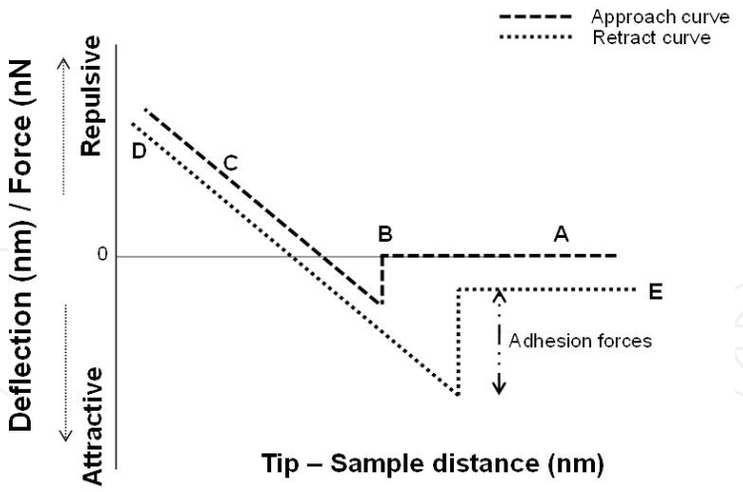

Figure 2. Schematic representation of idealized FD curves showing the approach and retract curve. A: the tip is approaching the sample surface; B: van der Waals attractive forces are experienced resulting in a snap-to-contact of the tip with the sample and indentation; C: deflection of the tip away from the sample; D: retraction of the tip; E: withdrawal of the tip from the sample. The larger the deflection of the cantilever, the stiffer the sample (see the slope of part C).

be retrieved from the FD curves that can be measured at slow rate [force-volume (FV)] [10], at high rate [11], via pulsed-force mode [12], peak force [13] or from the change in resonance frequency of the cantilever (contact-resonance AFM) [14] and by amplitude modulation [15]. Other mechanical properties that can be derived from FD curves are visco-elasticity, adhesion forces and energy (the area of the attractive part of the retract FD-curve) [16]. Additionally, FD-curve modifications induced by electrostatic charges can be investigated [17]. Electrical signals based on the conductivity through sample and tip may be monitored as well while the tip is moving over the sample [9]. It may be noticed that for mechanical studies with lateral resolution a sharp silicon or silicon nitride tip can be used but a spherical, colloidal probe may render more specific data on material-material mechanical interactions like forensically relevant adhesion interactions between gunshot and explosive residues and textile fibers [18].

3. Forensic potential of AFM imaging

As demonstrated in several studies, little research has been carried out into the forensic possibilities of AFM imaging [7, 18]. Subjects that have been investigated concern human hair analysis [19–24], document forgery [25–28], textile fibers [29, 30], fingermarks [31], gunshot and explosive residues [32, 33]. It is important to discriminate between those studies that have actually used this technique from a forensic point of view from those that employed AFM only to examine materials that may be present as traces at a crime scene. In case of forensic traces relevant micro- to nanosized regions are not visible at macro-level and thus difficult to detect. Even though AFM is a minimally invasive technique, an important condition for the preservation of evidence, the small scan area of usefully not more than 100 × 100 μm strongly limits a forensic application. In this respect, HRTEM/SEM mediated investigations could be more

useful if it were not that the required sample treatments for electron microscopy imaging have been proven responsible for surface modifications of the samples [34]. Also, electron microscopes operate in the majority of cases in high vacuum conditions. Atomic force microscopy does not require any specific form of sample preparation and operates in ambient conditions. In this section, important (potential) forensic applications of AFM imaging will be introduced and analyzed based on key articles from the field. In comparison with other currently available techniques, the value of AFM imaging to a CSI will be explored.

3.1. Hair analysis

Forensic hair analyses may be used for genotyping but also to provide information on past drug exposure. Current forensic hair analyses are mostly performed with ultra-high performance liquid chromatography–tandem mass spectrometry (UHPLC–MS/MS). Most of the general hair examinations with AFM imaging focused on the influence of chemicals, as for instance present in hair care products, on the surface structure of hair. Durkan *et al.*, for instance, showed a reduction in hair surface roughness after washing with a number of shampoos to typically below 10 nm (AFM Cambridgenano CN6000 SPM). This reduction was proven to be directly related to the type of product used [19]. In some cases, isolated deposits were left behind but how long they remained visible was, unfortunately, not investigated. Actual toxicological hair investigations using AFM imaging have not been reported so far. However, unless combined to Raman spectroscopy AFM may not be able to give a chemical identity of drugs or other hair deposits and therefore just play a minor role in toxicological hair investigations. Another difficulty of AFM imaging in a forensic hair examination is lack of a reference hair sample with representative physical properties. Variations in characteristics depend on the origin of the hair, the region within the origin (thus the age of the hair), differences in the hair producing follicles, environmental conditions and personal care habits. This subject has also been acknowledged by Gurden *et al.* in 2004 (AFM NanoScope IIIa; spring constant 0.06 N/m; loading force 3.6 nN) who tried to solve this problem with a classification of hair properties based on several cuticular descriptors calculated from the height images of various hair parts [21]. These cuticular descriptors provide a range of information on hair surface properties, and thus the possibility to correlate hair structure characteristics to environmental conditions the hairs have been exposed to. The forensic relevance of this has never been established but probably requires a more extensive database including not only imaging data but mechanical hair properties as well. Jeong *et al.* have given an interesting contribution to this subject by studying the effects of aging on normal Korean hair diameter and surface features with AFM (AFM NANOStation II; non-contact mode; frequency 146–236 kHz; spring constant 1–98 N/m) [23]. Any information that may contribute to estimating the age of a forensic trace is extremely valuable. The value of this lies in the fact that a trace deposition time can link a suspect to the time a crime has been committed. Interestingly, Jeong *et al.* discovered an increase in hair diameter in the first 20–30 years followed by a decrease with further age increase. For the cuticular descriptors, surface roughness increased also significantly with age. However, the presented results showed a large variation and thus low precision. It may be noticed that gender had no influence on the hair diameter of the Korean participants. The hair surface area studies of Tomes *et al*. with both SEM and AFM (AFM

Veeco; resonance frequency 300 kHz; spring constant 42 N/m) resulted in only little difference in quality of surface profiles obtained with these techniques [22]. For forensic hair imaging, the minimally invasive AFM technique may thus be preferred over SEM even though large hair surfaces may limit its effectiveness. The forensic relevance of the preservation of evidence weighs in this case heavier.

3.2. Document forgery

Document forgery involves the illegal altering, erasing or extension of its contents. The minimally invasive character of AFM imaging when compared to SEM fits well to this subject. Competitive less invasive techniques in this case are FTIR, Raman spectroscopy, near infrared hyperspectral imaging and digital technologies [35–37]. With respect to this subject, it is interesting that the study of Kasas *et al.* (Nanoscope IIIa) on line crossings produced with dot matrix printers and different ball-point pens on plain paper reported qualitatively the same or better AFM results when compared to SEM. Similar superior AFM quality over SEM in crossing line investigations has been reported by Chen *et al.* [27]. They demonstrated different roughness and maximum height values for commonly used paper (duplicator, copper printing, glassine and Kraft paper) samples whereby crossing lines were applied with three different types of oil-based pens (AFM Bruker; resonance frequency: 146–236 KHz; spring constant: 21–98 N/m). However, the number of scans in the 5×5 μm areas and the number of these spots were not given and significances in paper surface roughness could therefore not be given. Additionally, the authors provided amplitude images. These types of images normally show how the tip is deflected when encountering the sample's topography while the feedback system is trying to keep the amplitude constant. Because the deflection and amplitude images are actually the error signals, good amplitude (deflection) images will only be obtained in case of minimized deflection signals. Although this research proved the usefulness of AFM imaging to detect crossing lines in general, the overall paper surface roughness could hamper the detection of erased, partially erased streaks or slightly printed ink patterns. It is also important to realize that changes in height profiles of ink streaks on documents may result from absorption of the ink by the paper substrate. The impact of this phenomenon may vary for different types of paper and hinder a correct interpretation of the height images. Moreover, when only AFM imaging is applied in these types of investigations a clear evidence of counterfeit can never be provided. A chemical identification of the ink with for instance Raman spectroscopy is thereby indispensable to deliver the final crucial decisive information. A combination of AFM and Raman spectroscopy has therefore more forensic potential as demonstrated by Bradao *et al.* [28]. This investigation focused on the authentication of banknotes (US dollar, Euro and Brazilian real) on the basis of asymmetry and kurtosis for the evaluation of paper roughness. Based on these parameters AFM (spring constant 42 N/m, resonance frequency 285 kHz) could, in most of the cases, discriminate the paper that was used for the counterfeiting compared to that of the authentic banknote (based on scans from different banknote locations). As stated by Ellen, AFM imaging may provide useful information on crossing lines and thus on document forgery and the order of text application [26]. However, further research is warranted to confirm the same degree of usability for rougher paper or documents that have been exposed to extreme environmental conditions. Moreover, current

optical document examinations also focus on the chemical identity of crossing. The chemical heterogeneity that could be present in fraudulent documents could be well characterized with AFM phase imaging particularly in combination with infrared or Raman spectroscopy for chemical ink analysis.

3.3. Textile fibers

Current forensic textile investigations comprise microscopic, chemical and/or mechanical analyses. Although the value of forensic textile investigations concerns more, the mechanical properties of textile fibers under various environmental and weathering conditions [29]. AFM height images may deliver height, valley and mean square roughness values for different types of textiles. This subject has been investigated by Canetta *et al.* (JPK Bio AFM, Au-coated Si_3N_4 cantilever, spring constant: 0.03 N/m) in a study on environmentally stressed and weathered textile fibers [30]. An important result of this research is that the surface roughness differed significantly for all investigated textile fibers (natural cotton, wool and man-made viscose) and that it showed a time and environment dependent increase. Atomic force microscopy imaging may thus be used to distinguish the effect of different environmental effects on fibers and is thereby complementary to other microscopy techniques like scanning SEM and environmental scanning electron microscopy (ESEM). However, a forensic textile investigation requires also information on the chemical identity of textile fibers. Additional noninvasive techniques such as surface-enhanced Raman scattering, Raman microspectroscopy, FTIR or photodiodearray spectrophotometry are therefore still needed. As these techniques can provide both nature and color of the textile fibers [38], AFM imaging will not play a crucial role in forensic textile investigations. Unless combined to Raman spectroscopy, AFM imaging can only add complementary information on textile characteristics and degradation patterns.

3.4. Fingermarks

A fingermark is an impression of friction ridges of a human finger that consists of exogenous and endogenous compounds. In a CSI visualization of latent fingermarks is important because the patterns of ridges of a human fingermark are very characteristic and therefore a powerful biometric feature for a person's identification. A chemical identification of the fingermark components and their metabolites render additional donor information such as personal habits and health condition. The various physical, chemical and instrumental techniques [39–43] for fingermark visualization and analysis focus on improving the contrast between the ridges and the surface underneath, surface characteristics and the presence and identification of particular contaminants [44, 45]. The subject of age determination of a fingermark is also with respect to forensic fingermark research an important but not yet solved issue [46–48]. Atomic force microscopy imaging could highlight specific details of fingermark ridges and substrate surface provided that the roughness of the surface on which the fingermark was deposited does not increase the height of the fingermark ridges. This problem was indeed experienced in the study of Goddard *et al.* (AFM Veeco; resonance frequency 250–350 kHz; spring constant 20–80 N/m) [31]. In their study that focused on localized brass surface erosion processes in relation to fingermark ridge evaluation, the authors noticed how the high roughness of the brass

surface in a 70 × 70 μm scan area hampered the analysis of the ridges of a fingermark. In this particular research, these problems were solved by successfully polishing the brass surfaces. However, as stated by the authors themselves, this solution is far from realistic. Apart from the obstacle the surface roughness is giving, the inability of AFM to provide chemical information on the components of a fingermark further limits its forensic usefulness. Spectroscopy techniques that operate in a nondestructive manner seem to have more value in case of forensic fingermark examinations. Vibrational spectroscopy techniques like FTIR and conventional Raman are examples of methods that offer in a nondestructive manner a specificity for molecular identification that is comparable to mass spectrometry [41, 43]. The latter has nevertheless excellent selectivity and sensitivity in identifying unknown fingermark components but is highly destructive. Even AFM phase imaging cannot offer similar forensic effectiveness. This type of imaging can, unhindered by surface roughness, admittedly provide information on different materials and provide physicochemical mapping of exogenous substances present on fingermarks (for instance, gunshot or explosive residues or compounds that can be associated with sexual assaults) but fails in chemically identifying them. There is, however, still one application of AFM imaging that remains to be explored but could be potentially interesting in a forensic examination, the investigation and deconvolution of overlapping fingermarks and/or bloodstains.

3.5. Gunshot and explosive residues

Inorganic gunshot and explosive residues can provide important information in the forensic reconstruction of shooting incidents and are usually analyzed with neutron activation analysis (NAA) [49], atomic absorption spectrometry (AAS)-based methods [50, 51], inductively coupled plasma (ICP) [52], and SEM combined to energy dispersion analysis (SEM–EDX) [53]. Organic gunshot and explosive residues can be analyzed with gas chromatography (GC), GS-MS, or HPLC [54]. Additionally, time-of-flight secondary ion mass spectrometry (TOF–SIMS), ablation-ICP/MS and Raman micro-spectroscopy have been reported for both inorganic and organic gunshot and explosive residue characterization [55, 56]. To clarify the chemical identity of these residues, it is an extremely important element in CSIs that involve firearms. Consequently, AFM imaging will only have any value when combined to one of the indicated techniques. Such a combination of technologies has been reported to be successful to evaluate shooting distances based on the shape and size of GSR (Quesant Q-Scope 250 Nomad) [57]. D'Uffizi *et al.* explored micromechanical and micromorphological features of gunshot residue particles deposited on bullets and hands of a shooter and collected with double-sided tape. In combination with SEM-energy-dispersive spectroscopy and selected-area X-ray photoelectron spectroscopy, the role of AFM height and phase imaging in this investigation was only modest [32]. The only forensic gunshot and explosive investigation in which AFM imaging could provide sufficiently powerful information regards physicochemical characterization of gunshot and explosive residues that have been detected on hairs and in-between the ridges of fingermarks as demonstrated in several publications [21, 33]. In this respect, the study of Oxley *et al.* (Digital Instrument Dimension 31,000) proved that various chemical hair treatments (water, acetonitrile, KOH and $KMnO_4$) all resulted in a decrease in surface roughness. However, no information was given on the recovery time, thus the duration

of the observed decrease in roughness [33]. Moreover, finding the right location will still be difficult and time-consuming.

4. Forensic potential of force spectroscopy

In contrast to the limited value of AFM imaging in a CSI, FS can in fact play a crucial role in these investigations. The power of this AFM application concerns the possibility to measure forces at the nano-level and consequently calculate mechanical characteristics of materials and changes of these properties over time. Changes in mechanical characteristics of forensic trace material as function of time render the possibility to estimate the age of the trace. Yet there is little forensically mediated research on this subject. Investigations in this area have mainly focused on age determination of bloodstains [58–61] and to a lesser extent on hair [19, 20, 23, 62, 63], gunshot and explosive residues, [64] and pressure sensitive adhesives [65–67]. Based on key articles from the field, the application of FS in forensic hair, gunshot and explosive residue and pressure sensitive adhesives examinations will be discussed followed by more extensive attention to age determination of bloodstains.

4.1. Hair

As demonstrated by Durkan *et al.* force measurements (AFM Cambridgenano CN6000 SPM; spring constant 0.2 N/m) proved 20% increase in adhesive force and four times higher adhesion energy on hair deposits as compared to the bare hair surface with 6 nN adhesion force. The hair deposits in this study resulted from washing of the hairs with various shampoos. No data were available on statistical significance of these findings. More forensically interesting is the study of Jeong *et al.* that demonstrated the usefulness of AFM force measurements by showing age-dependent hair stiffness. The stiffness increased up to 30 years and then decreased again. The average adhesion force of the hairs, however, showed no age dependence. As also noticed by the authors, their data may not be representative for all hairs and hair parts. Force-distance and friction measurements between individual hair strands have been documented by Max *et al.* for direct quantification of hair-hair (other types of fiber) interactions in the range of 10–100 mm diameter (AFM Atomic Force F&E, MFP-3D; spring constant 1.2–8.5 N/m) [62]. DelRio and Cook have also provided interesting data of hair samples (untreated virgin hairs and conditioned and bleached hairs) [18]. They reported an indentation modulus of 2.4 $\pm$ 1.1 GPa and 1.8 $\pm$ 0.9 GPa for respectively the virgin and the bleached hairs. For the conditioned hairs, the modulus of indentation varied between 0.05 and 0.5 GPa depending on the position along the hair. All the measurements were performed on a 5 by 5 μm area but the number of indentations was not mentioned. Although all these investigations are interesting from a physical point of view, the forensic usefulness of mechanical hair parameters will be limited because of the numerous environmental and personal conditions affecting these parameters and thus the accuracy of the overall measurement. However, modeled in a Bayesian network, mechanical properties may be related to environmental conditions and used to calculate complex likelihood ratios and thus increase their usefulness in a CSI.

4.2. Gunshot and explosive residues

Apart from the topography of organic and inorganic particles present in gunshot residues and explosives, mechanical properties of these particles have a forensic value as well. With respect to this subject, Xu *et al.* have described an interesting nanoscale characterization of mock explosive materials, a study that fully explored the technical options of dynamic AFM such as phase imaging, force volume imaging, and Kelvin probe force microscopy (KPFM) with resonance enhancement (AFM Asylum Research MFP-3D AFM; spring constant 10.97 N/m; resonance frequency 147.53 kHz) [64]. Physical properties of components of explosive residues such as the density of the simulant, simulant to the explosive HMX and polymeric binder were mapped over 10×10 μm areas to understand the formation of hotspots and their local structure in relation to the processing method. This enabled mapping of local mechanical dissipation, elastic modulus, adhesion and the "effective" local dielectric constant of a mock explosive 900-21 sample (mechanical substitute for the plastic-bonded explosive PBX 9501). The authors used the phase lag between the excitation force and tip response for a nanoscale quantitative analysis of their sample and emphasized the importance of measuring this phase lag. To make the phase images more useful for quantitative mapping, conversion into energy dissipation maps was included. If the amplitude of the cantilever is kept constant, the phase shift is related to the energy dissipated in the tip-sample contact and phase data can thus provide energy dissipation maps [68]. The energy dissipation during one oscillation cycle by the tip on the sample was calculated according to the well-established method described by Martinez and Garcia [69]. To create adhesion and YM maps, FV mapping was employed based on Hertz contact model calculations. When compared to energy dissipation, adhesion or YM maps, the dielectric property map revealed more localized spatial features: fine and large crystals appeared to have the same dielectric constant while the binder region was characterized by a much higher dielectric constant. This study clearly demonstrated AFM multiparameter functionality resulting in a variety of physicochemical properties of compound mixtures. Particularly, the interfacial regions between crystalline zones of complex composite materials such as explosive residues were indicated as important areas where impurities, unreacted molecules, additives and binders form a heterogeneous structure. The study of DelRio and Cook also investigated adhesion forces of explosive particles on different fabric types using a colloidal probe [18]. The results showed for two fabrics similar modulus of indentation (29.0 ± 8.0 MPa for cotton and 30.7 ± 7.0 MPa for rayon) that differed from the values given in the literature (3 and 11 GPa for respectively cotton and rayon fibers) [70]. The authors ascribed the differences to variations in surface roughness and work of adhesion. This example illustrates the difficulty in quantifying mechanical properties based on AFM and determining the "true" value of a mechanical property. Some of the choices that can be made for in a given AFM measurement and the probes may influence the outcome of mechanical measurements and thus need to be correctly interpreted to insure the forensically desired accuracy and precision.

4.3. Pressure sensitive adhesives

Pressure sensitive adhesives (PSA) usually consist of a polymeric base with appropriate plasticizers and tackifiers and are, unfortunately, also employed in criminal activities such as assault, rape and hijacking to immobilize and blindfold victims and in the preparation of

homemade explosives. Typically, PSA investigations involve physical fiber characterization and chemical analysis of the adhesive additional to the search for fingermarks and DNA. A physical fit of free tape ends may constitute important evidence in the reconstruction of a crime and link a suspect to a scene of crime [71]. Current methods for PSA examinations of physical characteristics include polarized light microscopy, GS-MS [72], FTIR [72, 73], SEM [74], X-ray fluorescence spectrometry (XRF) [75], and ICP [76]. As PSA manufacturing and effectiveness depends on the cohesive and viscoelastic properties of the applied polymers, AFM may certainly play a role in forensic PSA examinations. In 2000, Paiva *et al.* applied AFM (AFM Autoprobe M5) in a PSA investigation for surface adhesion measurements on 7 months old polyethylene-propylene blends with different concentrations of the tackifier n-butyl ester of abietic acid [65]. A two-phase morphology was found for the blends at compositions exceeding 15 wt% tackifier. This resulted in two different types of behavior as demonstrated via nanoindentation measurements: a viscoelastic response in the tackifier-rich domains versus a more highly dissipative response in the matrix. In 2001, the same group used AFM to investigate PSA aging [67]. Apart from the polyethylene propylene/n-butyl abietate blends combinations of polyisoprene/n-butyl abietate and polyisoprene/pentalyn H were investigated after 2 weeks and 18 months with various tackifier concentrations. The microindentations in their study used a glass hemisphere probe (3 mm in diameter) and a maximum load of 25 mN while the nanoindentations were performed with a conical tip with a curvature radius of 10 nm. Adhesion measurements provided information on blend changes over time. While these changes appeared to be significant for the miscible polyisoprene/n-butyl abietate and polyisoprene/pentalyn H systems adhesion properties were not affected for the immiscible polyethylene propylene/n-butyl abietate samples. Moreover, adhesive stiffness revealed a more pronounced increase (elasticity reduction) as function of the tackifier concentrations in the miscible systems than in the immiscible system. This stiffening degrades the adhesive effectiveness of the films that could prove an interesting feature in a forensic investigation. Canetta *et al.* also presented different nanostructural and nanomechanical properties of a variety of adhesive tapes: three visually indistinguishable different, transparent OPP packaging tapes, the visually distinguishable brown packaging, and green electrical insulation tape (AFM NTEGRA; spring constant 45 N/m; resonance frequency 330 kHz) [66]. All tapes showed the existence of two phases: a hard low energy dissipative phase and a soft phase which exhibits more energy dissipation. The authors correctly noticed that in case of adhesive tapes with dispersed regions of higher and lower viscosity, the interaction of the AFM tip with the surface may vary. Consequently, less energy will be dissipated on surface regions with lower viscosity while in the more viscous areas enhanced energy dissipation occurs. For both the visually distinguishable and indistinguishable tapes, AFM measurements demonstrated statistical differences in the maximum adhesive force of the particles to the tip, the maximum distance of deformation of these particles and the adhesion energy. Atomic force microscopy can certainly give relevant nanomechanical information in a forensic PSA investigation that may not easily be clarified with other available techniques provided that the effect of environmental conditions on PSA is documented as well. Paiva *et al*. have also made a start with this and proved a decrease of elastic modulus with increasing relative humidity, estimated with Hertzian contact mechanics (Autoprobe CP scanning probe microscope operating in lateral force microscopy mode using the signal access module) [65].

4.4. Age determination of bloodstains

The most interesting forensic application of FS concerns undoubtedly the estimation of the age of a bloodstain at a crime scene. The need for estimating the deposition time of a trace of blood, linking a suspect to the time a crime has been committed, has attracted much attention worldwide over the years. Although many studies have focused on blood as the key trace at a crime scene, it is currently still not possible to provide an accurate determination of the age of a bloodstain. Except for hyperspectral imaging (HSI), technologies explored were all characterized as invasive and thus less attractive for forensic applications. Even though HSI is a promising technology deviations of the true age of bloodstains compared to the age determined with HSI already increase within a few days (for an actual age of 2 days, the absolute error is 2.7 days) [77]. An innovative and minimally invasive method for age determination of blood traces at a crime scene is thus highly needed. Force spectroscopy could provide estimations for bloodstain ages based on temporal changes in the elasticity of red blood cells (RBCs) [7, 8, 58–61]. One of the first FS researches related to this subjects was performed in 2007 by Strasser *et al.* (AFM Topometri Accurex; spring constant 80 N/m; resonance frequency 405 kHz) [59]. However, indentation areas were not correlated to specific RBCs, and thereby the condition of elasticity also neglected. On the contrary, the more extensive study of *Wu et al.* (AFM Veeco Autoprobe CP Research; frequency 72–96 kHz; spring constant 3 N/m (tapping mode); frequency 255–315 kHz; spring constant 0.9 N/m (contact mode)) showed a time-dependent, surface-dependent (glass and mica) and temperature-dependent (controlled 25°C, 76% humidity vs. uncontrolled outdoor 21–34°C, 38–87% humidity) increase of surface adhesive forces of RBCs between 5 and 30 days [58]. This result is indicative for an increase in stiffness of these cells over time. Chen and Cai (AFM AutoProbe CP; spring constant: 2.8 N/m) also observed time-dependent cellular changes in blood cells on a mica carrier in air [61]. Apart from the effects of temperature and humidity on the elasticity of RBCs, the influence of drugs has been investigated as well. The extensive study of Girasole *et al.* (contact mode spring constant 0.032 or 0.064; tapping mode spring constant 5 N/m) demonstrated that in vitro treatment of RBCs with the drug nifedipine, used in cases of cardiovascular disorders, caused dramatic morphological cellular changes that depended predominantly on the drug concentration and to a lesser extent on the exposure time [60]. The YM values calculated for the nifedipine-treated cells compared to control, native dehydrated RBCs, phenylhydrazine and formalin treated cells were respectively 96±14 kPa, 98±17kPa, 150±23kPa and 191±28kPa. Additional to the YM and shape of RBCs the authors emphasized the importance of other smaller, though significant age markers that can be found on the surface of RBCs such as, for example, spicules and crenatures. The YM measurements in this study were carried out carefully using the Hertz model adjusted for a four-sided pyramidal shape of the indenter as given by Sneddon [78] and Bilodeau [79] (see Eq. 1), a maximum load of close to 2.5 nN and an observed indentation depth of 50–60 nm.

$$F = \frac{C_0 2\delta^2 E}{\pi(1-\nu^2)\tan\alpha} \tag{1}$$

In this equation, F is the applied force (N), E is the YM (Pa), ν is the Poisson's ratio (typically 0.5 for elastic bodies), α is the apical tip angle and the coefficient, C_0 (1.46) is the specific

contribution of Bilodeau in the case of pyramidal tips. After the study of Girasole in 2012, it still took approximately 5 years before Smijs and Galli paid serious attention to the age determination of bloodstains using FS (AFM JPK instruments AG; frequency 300 kHz; spring constants 25.2–67.5 N/m) [8]. They applied FS combined to the Hertz model (see Eq. 2) to investigate the elasticity of randomly selected RBCs from the peripheral zone of 4- to 8-day-old bloodstains under controlled laboratory conditions.

$$F = \frac{4}{3}\frac{E}{1-\nu^2}\sqrt{r}\cdot\delta^{\frac{3}{2}} \tag{2}$$

In this equation, F represents the applied force (N), r the tip radius (m), E the Young's Modulus (Pa), ν the Poisson ratio and δ the deformation at maximum load (m). Special attention was paid to the condition of the silicon probes when continuously used to indent RBCs. An important conclusion of this study was that, based on 256 × 256 indentations/RBC, the elasticity of six RBCs from a 5-day-old bloodstain appeared homogenous over the cell (see **Figure 3A**) with a mean Young's modulus of 1.6 ± 0.4 GPa (see **Figure 3B**). Differences in RBC YM were significant but because of the large number of YM, data significance is here mainly caused by the size of the sample rather than by the chosen level of significance and thus leading to the detection of extremely small differences. Moreover, the authors showed that the eta-squared (η^2) effect size appeared to be 0.065. This means that the spreading between the data was for only 6.5% caused by the RBC itself. At the same time, this finding illustrates the complexity of age determination of a bloodstain in a forensic setting where a variety of environmental as well intrinsic blood and bloodstain factors affect the stiffening of RBCs.

Then authors noticed extremely blunting of their silicon tip resulting from many RBC indentations (from the original radius of 8–200 nm after a total of two sapphire calibrations and six RBC (256 × 256/cell) indentations. The contact area thus changes resulting in differences in physics at that nano-level. The authors solved this problem by checking the tip's radius before

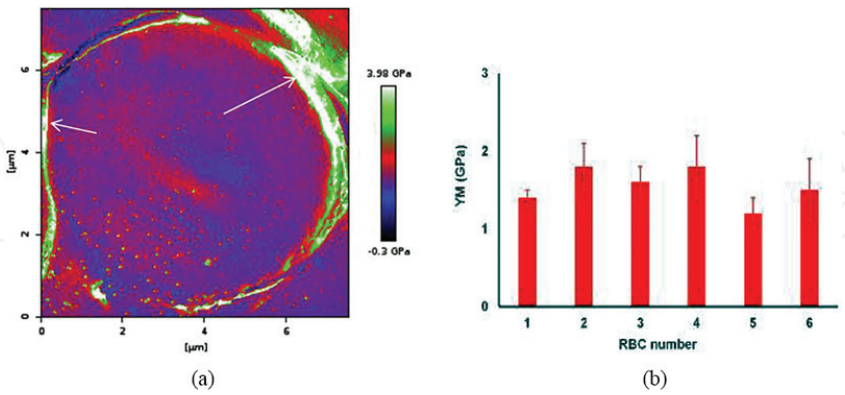

Figure 3. A representative example of an elasticity map (A) of a RBC and the mean YM (± SD, B) calculated for six RBCs. All RBCs were randomly chosen from the peripheral zone of a 5-day old bloodstain (6.5–7 mm in diameter, obtained from 3 μL capillary blood). The arrows in A indicate areas with artifacts probably based on a sharp fall of the tip at the edge of the RBC. The blood drop was passively deposited on a glass surface in a Petri-dish, dried (23.9 ± 0.5°C and 35 ± 7% relative humidity, n = 7) and measured after 5 days (27°C, 36% relative humidity). AFM (JPK Instruments AG) specifications: sapphire calibrated silicon tip (Olympus), spring constant 38.75 N/m; frequency 300 kHz; maximum load: 548 to 874 nN; indentation depths: 12 to 16 nm, [8]. Copyright © 2017 Smijs T.

and after RBC indentations. Up to a radius increase to approximately 100 nm, corrected radii were applied to the Hertz model. However, the authors rightfully recognized the shortcomings of this technique when it comes to an application on a real crime investigation with an unknown bloodstain with RBCs of unknown stiffness. A problem related to this, and also acknowledged by the authors, is the fast increasing stiffness of the RBCs over time and thus the need for an ever-stronger cantilever in order to assure indentation. These things were particularly noticed when RBC stiffness's of a bloodstain aging between 4 and 8 days was investigated (see **Figure 4A** and **B**).

AFM specifications for A: sapphire calibrated silicon tips (Micromash) with spring constants ranging from 45.5 N/m, 55.8 N/m and 55.1 for respectively day 4, day 5, 6 and day 7, 8; frequency: 300 kHz; maximum load: 3018 –3414 nN; indentation depths: 20–45 nm. Statistical data analysis (A) was performed with One-Way Repeated Measures Anova (IBM SPSS statistics 20) with a critical level of significance of $p = 0.05$ and based on YM values calculated with the Hertz model (Poisson ratio: 0.5; corrected radii: 20 nm for day 4 data, 70 nm for day 5 data, 133 nm for day 6 data, 75 nm for day 7 data, 130 nm for day 8 data) for 43,046 to 44,272 FD curves per cell. Given are the mean YM values/cell (± SD). Size effect η^2 for the factor day is 0.810. Calculated size effects for day 5 vs. 6, 6 vs. 7, and 7 vs. 8 were respectively 0.195, 0.727 and 0.597.

Presented mean YM in B (Hertz model, Poisson ratio: 0.5) were based on force measurements of three RBCs (equality variance proven, Mauchly's test) from the peripheral zone of the stain. AFM specifications: sapphire calibrated silicon tips (Olympus and Micromash) with spring constants of 25.2–67.5 N/m; frequency: 300 kHz; maximum load: 548–3905 nN; indentation depths: 8–63 nm.

Similar to other researchers, Smijs and Galli also found irregular values for the YM of RBCs between 2 and 4 days old. Wu *et al.* ascribed these fluctuations to a collapse of the cell, a feature that was also noticed by Girasole *et al.* Moreover, both Smijs *et al.* and Girasole noticed stiff spicules and crenatures on the surface of the RBCs [8, 60]. Smijs and Galli concluded from their study that additional experiments using similar but also realistic forensic conditions with

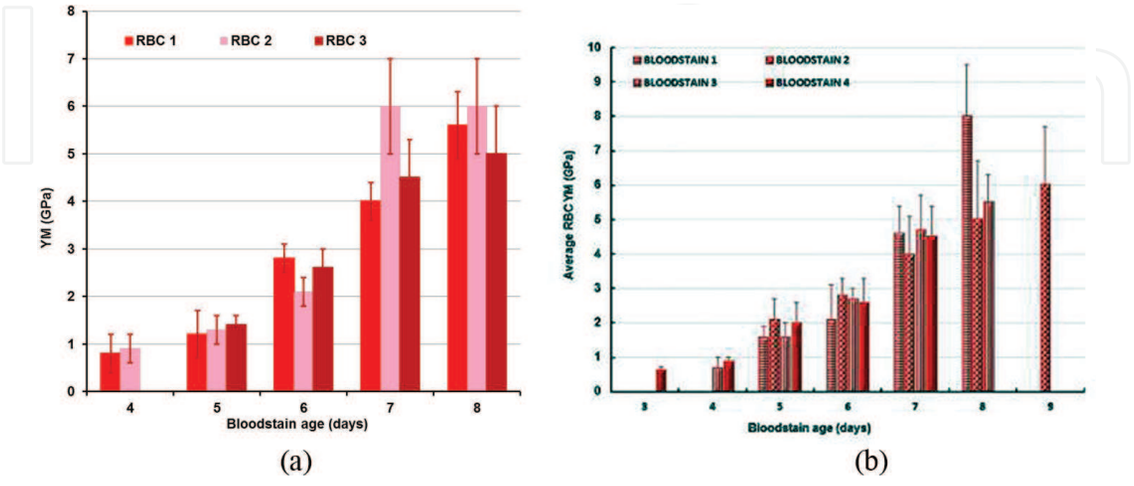

Figure 4. Representative changes in YM (± SD) of RBCs selected from the peripheral zone of a bloodstain between 4 and 8 days old (A) and changes in elasticity (YM ± SD) of cells from different 3- to 8-day-old bloodstains (B) [8]. Copyright © 2017 Smijs T.

optimized AFM probes, such as those with a more robust tip, so that the tip radius remains constant during the measurements, are needed. As the mechanism of RBC stiffening in a bloodstain is not completely known, it may be important to investigate not only the influence of external factors but also intrinsic RBC and bloodstain properties.

5. Conclusion

This chapter focused on the usefulness of AFM technology in forensic investigations. Important forensic examination subjects such as fingermarks, textile fibers, document forgery, gunshot and explosive residues and PSA have been discussed. Special attention was paid to age determination of bloodstains.

The forensic power of minimally invasive AFM is undoubtedly the ability to measure mechanical characteristics of trace materials such as elastic modulus, adhesion forces, energy dissipation and dielectric properties. Moreover, current AFM systems deliver synoptic mapping of these characteristics and FD curves for each pixel. Particularly, the ability to measure changes in mechanical properties of forensic traces over time makes this technology potentially interesting for a CSI. The increase of the YM of RBCs over time as measure for the age of a bloodstain is an excellent example of the forensic usefulness of FS. This information could provide valuable insights regarding the time of death of a victim or link a suspect to the scene at the time the crime was committed. Temporal forensic information can also be used to support or refute statements of victims, suspects and witnesses, especially when the defense states that the forensic evidence at hand is not related to the crime.

Less forensic value can be ascribed to AFM imaging. There are several reasons for this. The roughness of a surface on which a forensic trace has been deposited can hamper a proper examination of a height image. Although this problem could partially be solved by using phase imaging, many forensic trace characterizations require a chemical identity as well. Phase imaging will provide evidence only for the presence of different chemical substances but cannot identify them. However, AFMs equipped with optical microscopy and Raman spectroscopy or surface enhanced Raman spectroscopy may pave the way for AFM imaging as valuable tool for forensic examinations. Most promising in this respect is tip-enhanced Raman spectroscopy using a gold-coated atomic AFM tip-substrate system [80].

To grasp the forensic applicability of AFM in actual casework, additional research as well as laboratory and crime scene validation studies is required. The growing availability of fully automatic AFM systems that operate outside isolation cabinets brings a forensic AFM application closer.

Acknowledgements

The authors wish to thank Amu Hosseinzoi (BA.Sc.) for his tremendous commitment to a forensic application of AFM, particularly with respect to the RBC elasticity measurements.

Conflict of interest

There is no conflict of interest.

Thanks

Thanks to the great and close collaboration between Leiden Institute of Physics (LION, Leiden University, Leiden, The Netherlands) and the Netherlands Forensic Institute (the Hague, The Netherlands) we were able to write this chapter and perform our own forensic FS studies.

Author details

Threes Smijs[1,2]* and Federica Galli[2]

*Address all correspondence to: t.smijs@nfi.minvenj.nl

1 The Netherlands Forensic Institute, The Hague, The Netherlands

2 Leiden University, Leiden, The Netherlands

References

[1] Zou KN, Gui C, Gao Y, et al. Source identification of human biological materials and its prospect in forensic science. Fa Yi Xue Za Zhi. 2016;**32**:204-210. DOI: 10.1016/S1369-7021(09)70167-1

[2] Almog J. Forensic science does not start in the lab: The concept of diagnostic field tests. Journal of Forensic Sciences. 2006;**51**:1228-1234. DOI: 10.1111/j.1556-4029.2006.00256.x

[3] Pitkethly M. Nanotechnology and forensics. Materials Today. 2009;**12**(6). DOI: 10.1016/S1369-7021(09)70167-1

[4] Chen Y. Forensic applications of nanotechnology. Journal of the Chinese Chemical Society. 2012;**58**:828-835. DOI: 10.1002/jccs.201190129

[5] Inman K, Rudin N. Principles and Practice of Criminalistics—The Profession of Forensic Science. Boca Raton, Florida, USA: CRC Press; 2001

[6] Inman K, Rudin N. The origin of evidence. Forensic Science International. 2002;**126**:11-16. DOI: 10.1016/S0379-0738(02)00031-2

[7] Smijs T, Galli F, van Asten A. Forensic potential of atomic force microscopy. Forensic Chemistry. 2016;**2**:93-104. DOI: 10.1016/j.forc.2016.10.005

[8] Smijs T, Galli F. Forensic application of atomic force microscopy for age determination of bloodstains. Journal of Forensic Investigation. 2017;**5**:1-4

[9] JPK Instruments: Nano Wizard AFM handbook. version 2-2a; 2012. http://www.nanophys.kth.se/nanophys/facilities/nfl/afm/jpk/manuf-manuals/handbook-2.2a.pdf- [Accessed: March 17, 2016]

[10] Radmacher M, Cleveland JP, Fritz M, et al. Mapping interaction forces with the atomic force microscope. Biophysical Journal. 1994;**66**:2159-2165. DOI: 10.1016/S0006-3495(94)81011-2

[11] Sahin O, Magonov S, Su C, et al. An atomic force microscope tip designed to measure time-varying nanomechanical forces. Nature Nanotechnology. 2007;**2**:507-514. DOI: 10.1038/nnano.2007.226

[12] Rosa-Zeiser A, Weilandt E, Hild S, et al. The simultaneous measurement of elastic, electrostatic and adhesive properties by scanning force microscopy: Pulsed-force mode operation. Measurement Science and Technology. 1997;**8**:1333-1338. DOI: 10.1088/0957-0233/8/11/020

[13] Pittinger B, Erina N, Su C. Bruker Appl. Note. AN128; 2010. 1

[14] Rabe U, Janser K, Arnold W. Vibrations of free and surface-coupled atomic force microscope cantilevers: Theory and experiment. The Review of Scientific Instruments. 1996;**67**:3281-3293. DOI: 10.1063/1.1147409

[15] Garcia R, Proksch R. Nanomechanical mapping of soft matter by bimodal force microscopy. European Polymer Journal. 2017;**49**:1897-1906

[16] Leite FL, Mattoso LHC, Oliveira ON, et al. The atomic force spectroscopy as a tool to investigate surface forces: Basic principles and applications. In: Méndez-Vilas A, Diaz J, editors. Modern Research and Educational Topics in Microscopy. FORMATEX; 2007. pp. 747-757

[17] Boularas A, Baudoin F, Villeneuve-Faure C, et al. Multi-dimensional modelling of electrostatic force distance curve over dielectric surface: Influence of tip geometry and correlation with experiment. Journal of Applied Physics. 2014;**116**. 084106–1–084106-11. DOI: doi.org/10.1063/1.4894147

[18] DelRio FW, Cook RF. Quantitative scanning probe microscopy for nanomechanical forensics. Experimental Mechanics. 2017;**57**:1045-1055. DOI: 10.1007/s11340-016-0238-y

[19] Durkan C, Wang N. Nanometre-scale investigations by atomic force microscopy into the effect of different treatments on the surface structure of hair. International Journal of Cosmetic Science. 2014;**36**:598-605. DOI: 10.1111/ics.12161

[20] Wada H, Usukura H, Sugawara M, et al. Relationship between the local stiffness of the outer hair cell along the cell axis and its ultrastructure observed by atomic force microscopy. Hearing Research. 2003;**177**:61-70. DOI: 10.1016/S0378-5955(02)00798-0

[21] Gurden SP, Monteiro VF, Longo E, et al. Quantitative analysis and classification of AFM images of human hair. Journal of Microscopy. 2004;**215**:13-23. DOI: 10.1111/j.0022-2720.2004.01350.x

[22] Tomes C, Jones JT, Carr CM, et al. Three-dimensional imaging and analysis of the surface of hair fibres using scanning electron microscopy. International Journal of Cosmetic Science. 2007;**29**:293-299. DOI: 10.1111/j.1467-2494.2007.00382.x

[23] Jeong KH, Kim KS, Lee GJ, et al. Investigation of aging effects in human hair using atomic force microscopy. Skin Research and Technology. 2011;**17**:63-68. DOI: 10.1111/j.1600-0846.2010.00466.x

[24] Kim KS, Lee J, Jung MH, et al. Characterization of human ovarian teratoma hair by using AFM, FT-IR, and Raman spectroscopy. Microscopy Research and Technique. 2011;**74**: 1121-1126. DOI: 10.1002/jemt.21003

[25] Kasas S, Khanmy-Vital A, Dietler G. Examination of line crossings by atomic force microscopy. Forensic Science International. 2001;**119**:290-298. DOI: 10.1016/S0379-0738 (00)00458-8

[26] Ellen D. Scientific Examination of Documents Methods and Techniques. Boca Raton, USA: CRC Press; 2006

[27] Chen SZ, Tsai TL, Chen YF. Forensic application of atomic force microscopy questioned document. Journal of the Chinese Chemical Society. 2012;**59**:283-288. DOI: 10.1002/jccs.201100739

[28] Brandao JM, Almeida NSM, Dixini PVM, et al. Documentoscopy by atomic force microscopy (AFM) coupled with Raman microspectroscopy: Applications in banknote and driver license analyses. Analytical Methods. 2016;**8**:771-784. DOI: 10.1039/c5ay03128a

[29] Bruschweiler W, Grieve MC. A study on the random distribution of a red acrylic target fibre. Science and Justice. 1997;**37**:85-89. DOI: 10.1016/S1355-0306(97)72152-X

[30] Canetta E, Montiel K, Adya AK. Morphological changes in textile fibres exposed to environmental stresses: Atomic force microscopic examination. Forensic Science International. 2009;**191**:6-14. DOI: 10.1016/j.forsciint.2009.05.022

[31] Goddard AJ, Hillman AR, Bond JW. High resolution imaging of latent fingerprints by localized corrosion on brass surfaces. Journal of Forensic Sciences. 2010;**55**:58-65. DOI: 10.1111/j.1556-4029.2009.01217.x

[32] D'Uffizi M, Falso G, Ingo GM, et al. Microchemical and micromorphological features of gunshot residue observed by combined use of AFM, SA-XPS and SEM + EDS. Surface and Interface Analysis. 2016;**34**:502-506. DOI: 10.1002/sia.1348

[33] Oxley JC, Smith JL, Kirschenbaum LJ, et al. Accumulation of explosives in hair-Part 3: Binding site study. Journal of Forensic Sciences. 2012;**57**:623-635. DOI: 10.1111/j.1556-4029.2011.02020.x

[34] Poletti G, Orsini F, Lenardi C, et al. A comparative study between AFM and SEM imaging on human scalp hair. Journal of Microscopy. 2003;**211**:249-255. DOI: 10.1046/j.1365-2818.2003.01220.x

[35] Silva CS, Pimentel MF, Honorato RS, et al. Near infrared hyperspectral imaging for forensic analysis of document forgery. Analyst. 2014;**139**:5176-5184. DOI: 10.1039/c4an00961d

[36] Claybourn M, Ansell M. Using Raman spectroscopy to solve crime: Inks, questioned documents and fraud. Science and Justice. 2000;**40**:261-271. DOI: 10.1016/S1355-0306(00)71996-4

[37] Braz A, Lopez-Lopez M, Garcia-Ruiz C. Studying the variability in the Raman signature of writing pen inks. Forensic Science International. 2014;**245C**:38-44. DOI: 10.1016/j.forsciint.2014.10.014

[38] Meilero PP, García-Ruiz C. Spectroscopic techniques for the forensic analysis of textile fibers. Applied Spectroscopy Reviews. 2016;**51**:278-301. DOI: 10.1080/05704928.2015.1132720

[39] Koenig K, Girod A, Weyermann C. Identification of wax esters in fingermark residues by GC/MS and their potential use as aging parameters. Journal of Forensic Identification. 2011;**61**:652-676

[40] Bailey MJ, Bradshaw R, Francese S, et al. Rapid detection of cocaine, benzoylecgonine and methylecgonine in fingerprints using surface mass spectrometry. Analyst. 2015;**140**:6254-6259. DOI: 10.1039/c5an00112a

[41] Chan KL, Kazarian SG. Detection of trace materials with Fourier transform infrared spectroscopy using a multi-channel detector. Analyst. 2006;**131**:126-131. DOI: 10.1039/b511243e

[42] Dikshitulu YS, Prasad L, Pal JN, et al. Aging studies on fingerprint residues using thin-layer and high performance liquid chromatography. Forensic Science International. 1986;**31**:261-266. DOI: 10.1016/0379-0738(86)90165-9

[43] Connatser RM, Prokes SM, Glembocki OJ, et al. Toward surface-enhanced Raman imaging of latent fingerprints. Journal of Forensic Sciences. 2010;**55**:1462-1470. DOI: 10.1111/j.1556-4029.2010.01484.x

[44] Dutelle AW. Fingerprint evidence. In: An introduction to crime scene investigation. Burlington, USA: Jones and Bartlett Learning; 2014. pp. 169-202

[45] Bersellini C, Garofano L, Giannetto M, et al. Development of latent fingerprints on metallic surfaces using electropolymerization processes. Journal of Forensic Sciences. 2001;**46**:871-877. DOI: 10.1520/JFS15060J

[46] van Dam A, Aalders MC, Todorovski T, et al. On the autofluorescence of aged fingermarks. Forensic Science International. 2016;**258**:19-25. DOI: 10.1016/j.forsciint.2015.11.002

[47] Girod A, Ramotowski R, Lambrechts S, et al. Fingermark age determinations: Legal considerations, review of the literature and practical propositions. Forensic Science International. 2016;**262**:212-226. DOI: 10.1016/j.forsciint.2016.03.021

[48] Girod A, Xiao L, Reedy B, et al. Fingermark initial composition and aging using Fourier transform infrared microscopy (mu-FTIR). Forensic Science International. 2015;**254**:185-196. DOI: 10.1016/j.forsciint.2015.07.022

[49] Poppa P, Porta D, Gibelli D, et al. Detection of blunt, sharp force and gunshot lesions on burnt remains: A cautionary note. The American Journal of Forensic Medicine and Pathology. 2011;**32**:275-279. DOI: 10.1097/PAF.0b013e3182198761

[50] Aliste M, Chavez LG. Analysis of gunshot residues as trace in nasal mucus by GFAAS. Forensic Science International. 2016;**261**:14-18. DOI: 10.1016/j.forsciint.2016.01.034

[51] Aksoy C, Bora T, Senocak N, et al. A new method to reduce false positives due to antimony in detection of gunshot residues. Forensic Science International. 2015;**250**:87-90. DOI: 10.1016/j.forsciint.2015.03.006

[52] Abrego Z, Ugarte A, Unceta N, et al. Unambiguous characterization of gunshot residue particles using scanning laser ablation and inductively coupled plasma-mass spectrometry. Analytical Chemistry. 2012;**84**:2402-2409. DOI: 10.1021/ac203155r

[53] French J, Morgan R. An experimental investigation of the indirect transfer and deposition of gunshot residue: Further studies carried out with SEM-EDX analysis. Forensic Science International. 2015;**247**:14-17. DOI: 10.1016/j.forsciint.2014.10.023

[54] Taudte RV, Beavis A, Blanes L, et al. Detection of gunshot residues using mass spectrometry. BioMed Research International. 2014;**2014**:965403. DOI: 10.1155/2014/965403

[55] Coumbaros J, Kirkbride KP, Klass G, et al. Characterisation of 0.22 caliber rimfire gunshot residues by time-of-flight secondary ion mass spectrometry (TOF-SIMS): A preliminary study. Forensic Science International. 2001;**119**:72-81. DOI: 10.1016/S0379-0738(00)00421-7

[56] Abrego Z, Grijalba N, Unceta N, et al. A novel method for the identification of inorganic and organic gunshot residue particles of lead-free ammunitions from the hands of shooters using scanning laser ablation-ICPMS and Raman micro-spectroscopy. Analyst. 2014;**139**:6232-6241. DOI: 10.1039/c4an01051e

[57] Mou Y, Lakadwar J, Rabalais JW. Evaluation of shooting distance by AFM and FTIR/ATR analysis of GSR. Journal of Forensic Sciences. 2008;**53**:1381-1386. DOI: 10.1111/j.1556-4029.2008.00854.x

[58] Wu Y, Hu Y, Cai J, et al. Time-dependent surface adhesive force and morphology of RBC measured by AFM. Micron. 2009;**40**:359-364. DOI: 10.1016/j.micron.2008.10.003

[59] Strasser S, Zink A, Kada G, et al. Age determination of blood spots in forensic medicine by force spectroscopy. Forensic Science International. 2007;**170**:8-14. DOI: 10.1016/j.forsciint.2006.08.023

[60] Girasole M, Dinarelli S, Boumis G. Structure and function in native and pathological erythrocytes: A quantitative view from the nanoscale. Micron. 2012;**43**:1273-1286. DOI: 10.1016/j.micron.2012.03.019

[61] Chen Y, Cai J. Membrane deformation of unfixed erythrocytes in air with time lapse investigated by tapping mode atomic force microscopy. Micron. 2006;**37**:339-346. DOI: 10.1016/j.micron.2005.11.011

[62] Max E, Hafner W, Bartels FW, et al. A novel AFM based method for force measurements between individual hair strands. Ultramicroscopy. 2010;**110**:320-324. DOI: 10.1016/j.ultramic.2010.01.003

[63] Clifford CA, Sano N, Doyle P, et al. Nanomechanical measurements of hair as an example of micro-fibre analysis using atomic force microscopy nanoindentation. Ultramicroscopy. 2012;**114**:38-45. DOI: 10.1016/j.ultramic.2012.01.006

[64] Xu X, Mres J, Groven LJ, et al. Nanoscale characterization of mock explosive materials using advanced atomic force microscopy methods. Journal of Energetic Materials. 2015;**33**: 51-65. DOI: 10.1080/07370652.2014.889780

[65] Paiva A, Sheller N, Foster MD. Study of the surface adhesion of pressure-sensitive adhesives by atomic force microscopy and spherical indenter tests. Macromolecules. 2000;**33**: 1878-1881. DOI: 10.1021/ma990765v

[66] Canetta E, Adya AK. Atomic force microscopic investigation of commercial pressure sensitive adhesives for forensic analysis. Forensic Science International. 2011;**210**:16-25. DOI: 10.1016/j.forsciint.2011.01.029

[67] Paiva A, Sheller N, Foster MD. Microindentation and Nanoindentation studies of aging in pressure-sensitive adhesives. Macromolecules. 2001;**34**:2269-2276. DOI: 10.1021/ma0002343

[68] Stark M, Moller C, Muller DJ, et al. From images to interactions: High-resolution phase imaging in tapping-mode atomic force microscopy. Biophysical Journal. 2001;**80**:3009-3018. DOI: 10.1016/S0006-3495(01)76266-2

[69] Martinez NF, Garcia R. Measuring phase shifts and energy dissipation with amplitude modulation atomic force microscopy. Nanotechnology. 2006;**17**:S167-S172. DOI: 10.1088/0957-4484/17/7/S11

[70] Bunsell AR. Introduction to fibre tensile properties and failure. In: Handbook of Tensile Properties of Textile and Technical Fibres. Cambridge: Woodhead Publishing; 2009. pp. 1-17

[71] Katz E, Halamek J. Forensic Sciences: A Multidisciplinary Approach. Weinheim, Germany: Wiley-VCH; 2016

[72] Kumooka Y. Discrimination of rubber-based pressure sensitive adhesives by size exclusion chromatography. Forensic Science International. 2007;**171**:5-8. DOI: 10.1016/j.forsciint.2006.09.005

[73] Cui Y, Frank SG. Characterization of supersaturated lidocaine/polyacrylate pressure sensitive adhesive systems: Thermal analysis and FT-IR. Journal of Pharmaceutical Sciences. 2006;**95**:701-713. DOI: 10.1002/jps.20445

[74] Fang C, Lin ZX. Effect of propyleneimine external cross-linker on the properties of acrylate latex pressure sensitive adhesives. International Journal of Adhesion and Adhesives. 2015;**61**:1-7. DOI: 10.1016/j.ijadhadh.2015.04.009

[75] Sun ZW, Quan YK, Sun YY. Elemental analysis of white electrical tapes by wavelength dispersive X-ray fluorescence spectrometry. Forensic Science International. 2013;**232**:169-172. DOI: 10.1016/j.forsciint.2013.07.009

[76] Khalina M, Sanei M, Mobarakeh HS, et al. Preparation of acrylic/silica nanocomposites latexes with potential application in pressure sensitive adhesive. International Journal of Adhesion and Adhesives. 2015;**58**:21-27. DOI: 10.1016/j.ijadhadh.2014.12.007

[77] Edelman G, van Leeuwen TG, Aalders MC. Hyperspectral imaging for the age estimation of blood stains at the crime scene. Forensic Science International. 2012;**223**:72-77. DOI: 10.1016/j.forsciint.2012.08.003

[78] Sneddon IN. The relation between load and penetration in the Axi-symmetric Boussinesq problem for a punch of arbitrary profile. International Journal of Engineering Science. 1965;**3**:47-57. DOI: 10.1016/0020-7225(65)90019-4

[79] Bilodeau GG. Regular pyramid punch problem. Journal of Applied Mechanics. 1992;**59**: 519-523. DOI: 10.1115/1.2893754

[80] Meng L, Huang T, Wang X, et al. Gold-coated AFM tips for tip-enhanced Raman spectroscopy: Theoretical calculation and experimental demonstration. Optics Express. 2015;**23**: 13804-13813. DOI: 10.1364/OE.23.013804